PROCEEDINGS OF SCIENCE

Recent progress in the tensor renormalization group

Daisuke Kadoh[a,b,*]

[a] *Faculty of Sciences and Engineering, Doshisha University, Kyoto 610-0394, Japan*

[b] *Research and Educational Center for Natural Sciences, Keio University, Yokohama 223-8521, Japan*

E-mail: dkadoh@mail.doshisha.ac.jp, kadoh@keio.jp

The tensor renormalization group is a very attractive approach for numerically calculating lattice field theory. It does not suffer from the sign problem, and it is a method that enables calculation with an extremely large volume lattices and direct calculation of free energy. I report on recent developments in this field and clarify the problems to be solved in the future.

The 38th International Symposium on Lattice Field Theory, LATTICE2021 26th-30th July, 2021
Zoom/Gather@Massachusetts Institute of Technology

*Speaker

PoS(LATTICE2021)633

1. Introduction

The tensor renormalization group (TRG) is an promising approach for computing lattice field theory. It was originally proposed by Levin-Nave in 2007 [1] for analyzing the two-dimensional Ising model. Some improvements[2–6], higher dimensional algorithms [7–9] and algorithms for fermion theory[10–15] have been proposed so far. Since this method has no sign problem from the beginning, it is expected to be applied to important models for understanding the evolution of the early universe and the origin of matter, such as finite density QCD, supersymmetric theory, chiral gauge theory, theta vacuum and their real-time simulations.

The TRG was actually introduced into the study of quantum field theory in the last decade. So far, various models of lattice field theories have been investigated. In two dimensions, the TRG was applied to scalar field theory [16–22], Schwinger model[14, 23, 24], Gross-Neveu model[25], CP(N-1) model[26, 27], Wess-Zumino model[28] and related studies[29], gauge Higgs model[30], U(1) lattice gauge theory with theta term[31], 2d gravity[32] and SU(N) Yang-Mills theory[33, 34] and O(2) nonlinear sigma model[35]. In three dimensions, the TRG calculations were performed in Z_2 gauge theory[36], $O(2)$ model[37]. In four dimensions, scalar field theory[38, 39], and NJL model[40] and Z_2 gauge-Higgs model[41] were studied. Theoretical study related with quantum gravity are in Refs.[42–46] and other related studies are in Refs.[29, 47–52].

This paper reviews the recent progress in the TRG method, which is important in studying quantum field theory. In particular, we will give an overview of the handling of scalar fields, fermion fields, and gauge fields in the tensor network method. The developing high-dimensional algorithms are also reviewed.

The rest of this paper is organized as follows. In section 2, the Levin-Nave TRG method is reviewed. A tensor network representation of scalar field theory is introduced in section 3. After which, section 4 introduces the TRG method for lattice fermion theory. Section 5 describes a new method of calculating gauge theory by the TRG method. In section 6, the TRG approach to higher dimensional theories is presented. Finally section 7 presents summary and future outlook.

2. Tensor networks and the TRG

We begin with considering the TRG method in classical Ising model on two dimensional square lattice. Throughout this paper the lattice spacing a is set to $a = 1$ and lattice sites are labeled by d integers as $n = (n_1, n_2, \ldots, n_d) \in \Gamma_d$. The unit vector of the μ direction is denoted by $\hat{\mu}$. For later convenience, we denote a d-dimensional hyper cubic lattice as $\Gamma_d = \{(n_1, n_2, \cdots, n_d) | n_i \in \mathbb{Z}\}$.

Let σ_n be the spin variable that takes $\sigma_n = \pm 1$. The Hamiltonian is defined by $H = -J \sum_{\langle i,j \rangle} \sigma_i \sigma_j$ where $\langle i, j \rangle$ denotes all possible pairs of nearest neighbor sites. For simplicity, we take $J = 1$. The partition function is given as $Z = \mathrm{Tr}\, \mathrm{e}^{-\beta H}$ with the inverse temperature $\beta = 1/T$.

In order to define a tensor, we decompose the hopping term $\mathrm{e}^{\beta \sigma_i \sigma_j}$ as

$$\mathrm{e}^{\beta \sigma_i \sigma_j} = \sum_{I=0}^{1} W_{\sigma_i I} W_{\sigma_j I} \tag{1}$$

where $W_{\sigma I} = \sqrt{\cosh(\beta)}\sqrt{\tanh(\beta)}^{I}\sigma^{I}$ for $I = 0, 1$ and $\sigma = \pm 1$. Note that σ_i interacts with its nearest neighbor variable σ_j via the new index I which is defined on the link from i to j. This decomposition is applied to all the hopping terms. Then, in case of one-dimension, the partition function is expressed by $Z = \mathrm{tr}(T^N)$ where T is a transfer matrix defined by $T_{IJ} \equiv \sum_{\sigma=\pm1} W_{\sigma I} W_{\sigma J}$.

In two-dimensions, since the four hopping terms are stemmed from a site, a rank-4 tensor appears:

$$T_{ijkl} = \sum_{\sigma=\pm1} W_{\sigma i} W_{\sigma j} W_{\sigma k} W_{\sigma l}. \tag{2}$$

Thus we have a tensor network representation of Z as

$$Z = \mathrm{Tr} \prod_{n\in\Gamma_2} T_{x_n x'_n y_n y'_n}. \tag{3}$$

Here $x'_n = x_m$ for m is the nearest neighbor site of n in the positive x direction, and the same applies to y'_n. Here the trace of (3) denotes the summation of index that appears twice over all possible values of the index. Fig.1 shows (2) and (3) graphically. The form of (3) is kept in every renormalization step of tensor network, as shown below.

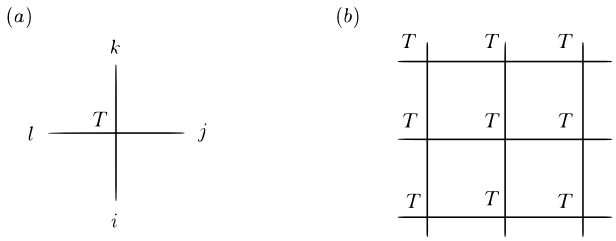

Figure 1: Tensor (a) and tensor network on 2d square lattice (b).

In the Levin-Nave TRG, the singular value decomposition (SVD) is used to renormalize the tensor network. The SVD of an $n \times n$ matrix M_{IJ} is given by

$$M_{IJ} = \sum_{a=1}^{n} \sigma_a U_{Ia} V^*_{Ja}, \tag{4}$$

where σ_a are singular values sorted in the descending order as $\sigma_1 \geq \sigma_2 \geq \cdots \geq \sigma_n \geq 0$ and U, V are unitary matrices. The SVD provides the best m-rank approximation of M for $m \leq n$ as $M_{IJ} \approx \sum_{a=1}^{m} \sigma_a U_{Ia} V^*_{Ja}$ truncating the summation range.

The rank-4 tensor T_{ijkl} can be decomposed by the SVD as $T_{ijkl} = \sum_{a=1}^{D^2} \sigma_a U_{ija} V^*_{kla}$ because it is a matrix regarding four tensor indices as the column $I = (i, j)$ or the row $J = (k, l)$. So we have an approximate decomposition of the tensor at even sites $(n_1 + n_2 \bmod 2 = 0)$ as

$$T_{ijkl} \approx \sum_{a=1}^{D} E_{ija} \bar{E}_{kla}, \tag{5}$$

where $E_{ija} = \sqrt{\sigma_a} U_{ija}$ and $\bar{E}_{ija} = \sqrt{\sigma_a} V^*_{ija}$. Similarly, at odd sites $(n_1 + n_2 \bmod 2 = 1)$, we have another decomposition,

$$T_{ijkl} \approx \sum_{a=1}^{D} O_{jka} \bar{O}_{lia}, \tag{6}$$

by identifying the tensor indices as the column $I = (j, k)$ or the row $J = (l, i)$ of the matrix to be decomposed. Fig.2 shows these decompositions. We should note that new index a actually runs from 1 to D^2 and in (5) and (6) the summations are truncated upto D.

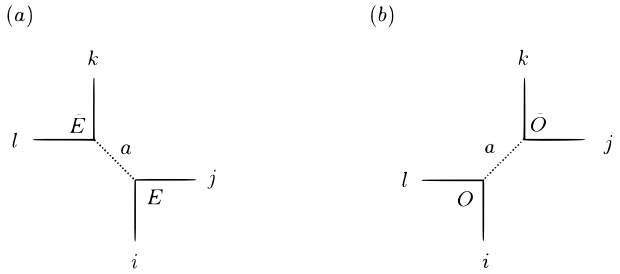

Figure 2: Decompositions of the tensor at even sites (a) and odd sites (b).

We define a renormalized tensor with new index as

$$T'_{abcd} = \sum_{i,j,k,l=1}^{D} E_{ija} \bar{O}_{jkb} \bar{E}_{klc} O_{lid}, \tag{7}$$

by integrating old indices i, j, k, l. From the construction, the partition function is again expressed as a tensor network of the form (3) with the tensor (7). Fig.3 shows a renormalization step of the Levin-Nave TRG, which is the transformation from T to T'. Thus we have a series of renormalized tensors from the initial tensor $T^{(0)}$ as $T^{(0)} \to T^{(1)} \to T^{(2)} \to \cdots$ by repeating above procedure again and again. If the tensor network is put on the periodic lattice of the size $2^N \times 2^N$, after $2N$ renormalizations Z is approximated by a single tensor $T^{(2N)}$ as $Z \approx \sum_{i,j=1}^{D} T^{(2N)}_{ijij}$

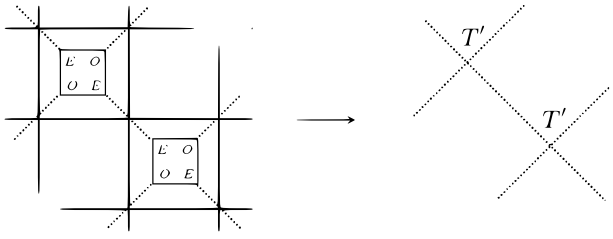

Figure 3: Decompositions of the tensor at even sites (a) and at odd sites (b).

The algorithm of the Levin-Nave TRG scales with $O(D^6)$. The computational cost can be reduced upto $O(D^5)$ using the randomized SVD. The systematic error derived from the finite D is

evaluated by changing D and investigating the D dependence of the result. In numerical calculation, we typically use $D \simeq 10 - 100$. In Fig.4 of Ref.[7], the free energy is obtained with good accuracy for $D = 24$.

3. Scalars

We consider a d-dimensional scalar field theory with a lattice action,

$$S_{\mathrm{B}} = \sum_{n \in \Gamma_d} \left\{ \frac{1}{2} \sum_{\mu=1}^{d} \left(\phi_{n+\hat{\mu}} - \phi_n\right)^2 + V(\phi_n) \right\}. \tag{8}$$

where a real scalar field ϕ and $V(\phi) = m^2\phi^2/2 + \lambda\phi^4/4$. The partition function is defined as

$$Z_{\mathrm{B}} = \int \mathcal{D}\phi e^{-S_{\mathrm{B}}(\phi)}, \tag{9}$$

where $\int \mathcal{D}\phi = \int_{-\infty}^{\infty} \prod_{n \in \Gamma_d} \mathrm{d}\phi_n$. Unlike the Ising model, a naive tensor of this theory has an infinite bond dimension because the field variable which is essentially the tensor index takes any real number. Therefore a discretization of the scalar field is needed to define a finite dimensional tensor.

The Gaussian quadrature rule is widely used to approximate an integral of the form $I = \int_{-\infty}^{\infty} dx\, f(x)$. If the integrand $f(x)$ has exponentially damping factors as $f(x) \sim \exp(-x^2)$, the Gauss-Hermite quadrature,

$$I \approx \sum_{x \in S_K} g_K(x) f(x), \tag{10}$$

approximates the integral well. Here S_K is the set of roots of the Kth Hermite polynomial $H_K(x)$ and $g_K(x)$ is a weight function defined by

$$g_K(x) = \frac{2^{K-1} K! \sqrt{\pi}}{(K H_{K-1}(x))^2} e^{x^2}. \tag{11}$$

The approximate expression (10) is expected to reproduce the original integral I in the large K limit. In actual numerical calculation, we numerically check the convergence of the result at large K.

Replacing each integral of the path integral by (10) as

$$\int_{-\infty}^{\infty} d\phi_n \to \sum_{\phi_n \in S_K} g_K(\phi_n), \tag{12}$$

we obtain an approximation of the partition function,

$$Z'_{\mathrm{B}} \equiv \sum_{\{\phi\}} \left(\prod_{n \in \Gamma_d} g_K(\phi_n) \right) \cdot e^{-S_B(\phi)}, \tag{13}$$

where

$$\sum_{\{\phi\}} \equiv \prod_{n \in \Gamma_d} \sum_{\phi_n \in S_K}. \tag{14}$$

$Z'_{\rm B}$ depends on K. Since $\exp(-S_B)$ decreases rapidly for large ϕ, $Z_{\rm B}$ is expected to be reproduced from $Z'_{\rm B}$ taking $K \to \infty$.

If we define a hopping term as

$$f(\phi,\phi') = (g_K(\phi)g_K(\phi'))^{\frac{1}{2d}} \exp\left\{-\frac{1}{2}(\phi-\phi')^2 - \frac{1}{2d}(V(\phi)+V(\phi'))\right\}, \tag{15}$$

we have

$$Z'_{\rm B} = \sum_{\{\phi\}} \prod_{n\in\Gamma_d} f(\phi_n,\phi_{n+\hat{1}}) f(\phi_n,\phi_{n+\hat{2}}) \cdots f(\phi_n,\phi_{n+\hat{d}}). \tag{16}$$

Note that f is a $K\times K$ matrix for $\phi,\phi' \in S_K$. Since f is a real symmetric matrix, we can decompose it as $f(\phi,\phi') = \sum_{A=1}^{K} e_A U_{\phi A} U_{\phi' A}$ by the SVD (Takagi's factorization) where e_A are singular values sorted as $e_1 \geq e_2 \geq \cdots \geq 0$ and U is a unitary matrix. Thus, for $\phi,\phi' \in S_K$, we have

$$f(\phi,\phi') = \sum_{A=1}^{K} W_{\phi A} W_{\phi' A} \tag{17}$$

where $W_{\phi A} = \sqrt{e_A} U_{\phi A}$.

An important point here is that (16) is very similar to the partition function of the classical Ising model except for the difference between $\sigma_n \in \{-1,+1\}$ and $\phi_n \in S_K$. So we can define a finite dimensional tensor using the same way as (1).

Thus a tensor network representation of the partition function can be obtained by using (17). For instance, in two dimensions, comparing (17) to (1), we find that $Z'_{\rm B}$ is expressed as the tensor network (3) with a tensor

$$T_{IJKL} = \sum_{\phi\in S_K} W_{\phi I} W_{\phi J} W_{\phi K} W_{\phi L}. \tag{18}$$

Once the tensor network representation is obtained, we can evaluate the numerical value of $Z'_{\rm B}$ using the TRG.

In two dimensions, the cost of the fist step of the Levin-Nave TRG scales with $O(K^6)$ instead of $O(D^6)$ because the bond dimension of (18) is K. Since $Z'_{\rm B}$ depends on K which is the number of discretized points, the convergence of results at large K should be checked numerically. In actual calculation, the value of K is often of $O(10)$ in two-dimensions, which is the same order of D.

Similar tensor network representations are obtained for many flavors and complex scalars. In Ref[19], two-dimensional complex scalar theory with finite chemical potential μ was studied by the TRG with the Gaussian quadrature. In this theory, it is expected that bulk observables such as the particle number density do not depend on μ below a critical value. This behavior is known as the Silver Braze phenomena which is closely related to the complex part of the action. Fig.4 of Ref.[19] shows the particle number density obtained by the TRG. The Silver braze phenomena is clearly observed. Therefore we find that the TRG properly works for theories with the sign problem.

4. Fermions

The partition function of fermion theory is also expressed as a tensor network. Since fermion fields are given by Grassmann numbers, the tensor index satisfies an anti commuting rule. The

tensor with such as anti-commuting index is called the Grassmann tensor [10]. Here, we introduce the Grassmann tensor and its tensor network following the notation of Ref.[15].

We consider a rank-N tensor $T_{i_1 i_2 \cdots i_N}$ with occupation numbers $i_n = 0, 1$ for $n = 1, 2, \ldots, N$. The Grassmann tensor of rank-N is formally defined as

$$\mathcal{T}_{\eta_1 \eta_2 \cdots \eta_N} = \sum_{i_1=0}^{1} \sum_{i_2=0}^{1} \cdots \sum_{i_N=0}^{1} T_{i_1 i_2 \cdots i_N} \eta_1^{i_1} \eta_2^{i_2} \cdots \eta_N^{i_N}, \tag{19}$$

where η_i $(i = 1, \cdots, N)$ are single-component Grassmann variables satisfying $\{\eta_i, \eta_j\} = 0$. The tensor $T_{i_1 i_2 \cdots i_N}$ is refereed to as a coefficient tensor of $\mathcal{T}$. Fig.4 (a) represents (19) where η_n are denoted by N external lines.

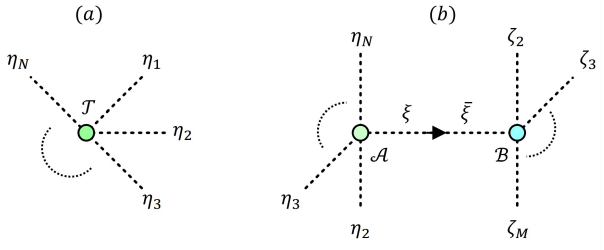

Figure 4: Grassmann tensor (a) and Grassmann tensor contraction (b).

We now set the rules for the Grassmann tensor contraction. The contraction has an orientation. Taking a contraction from η_k of $\mathcal{A}$ to ζ_l of $\mathcal{B}$, we define a Grassmann tensor C as

$$C_{\eta_1 \cdots \check{\eta}_k \cdots \eta_N \zeta_1 \cdots \check{\zeta}_l \cdots \zeta_M} \equiv \int d\bar{\xi} d\xi e^{-\bar{\xi}\xi} \mathcal{A}_{\eta_1 \cdots \eta_N} \mathcal{B}_{\zeta_1 \cdots \zeta_M} \Big|_{\eta_k = \xi, \zeta_l = \bar{\xi}}. \tag{20}$$

Here $\check{\eta}_k, \check{\zeta}_l$ mean that they are removed from the indices of C. Therefore the rank of Eq. (20) is $N + M - 2$. Fig.4 (b) show the Grassmann tensor contraction. The coefficient tensor of C is read from (20) as

$$C_{i_1 \cdots \check{i}_k \cdots i_N j_1 \cdots \check{j}_l \cdots j_M} = \sum_{m=1}^{2} A_{i_1 \cdots m \cdots i_N} B_{j_1 \cdots m \cdots j_M} \times (-1)^{m(i_{k+1} + \cdots + i_N + j_1 + \cdots + j_{l-1})} \tag{21}$$

replacing i_k, j_l with m in the RHS and the others unchanged. Here $\check{i}_k$ and $\check{j}_l$ are absent as the tensor index of the LHS. We find that there is an extra sign factor that comes from the Grassmann contraction rule.

We define a Grassmann tensor network as a product of Grassmann tensors whose indices are contracted under (20). Using the Grassmann contraction rule, matrix decompositions such as the SVD can be given as decompositions of a Grassmann tensor into two Grassmann tensors. Thus the TRG methods are easily transcribed to methods for Grassmann tensor networks.

In d dimensions, using this notation, we can represent the partition function of local fermion theory as a Grassmann tensor network. Let $\psi_{n,a}$ and $\bar{\psi}_{n,a}$ be fermion fields where $n \in \Gamma_d$ and an

index a corresponding to the spinor and flavor indices runs from 1 to N. We consider a general form of local lattice fermion action,

$$S_F = \sum_{n\in\Gamma_d} \bar{\psi}_n D\psi_n \tag{22}$$

with

$$D_{nm} = W\delta_{nm} + \sum_{\mu=1}^{d}(X_\mu)\delta_{n+\hat{\mu},m} + \sum_{\mu=1}^{d}(Y_\mu)\delta_{n-\hat{\mu},m}, \tag{23}$$

where X, Y, W are matrices with respect to a as X_{ab}, Y_{ab}, W_{ab}, and D_{nm} is also a matrix $D_{nm;ab}$. For the free Wilson fermion, we have

$$W_\mu = 1, \quad X_\mu = -\frac{\kappa}{2}\left(1-\gamma_\mu\right), \quad Y_\mu = -\frac{\kappa}{2}\left(1+\gamma_\mu\right). \tag{24}$$

The partition function is

$$Z = \int \left[\mathrm{D}\psi\mathrm{D}\bar{\psi}\right] \mathrm{e}^{-S_F}, \tag{25}$$

where $\left[\mathrm{D}\psi\mathrm{D}\bar{\psi}\right]$ denotes the standard fermion measure.

The partition function (25) can be expressed as a Grassmann tensor network:

$$Z = \mathrm{gTr}\left[\prod_{n\in\Gamma_d} \mathcal{T}_{\Psi_1(n)\cdots\Psi_d(n)\bar{\Psi}_d(n-\hat{d})\cdots\bar{\Psi}_1(n-\hat{1})}\right], \tag{26}$$

where gTr denotes the Grassmann contraction. Here the Grassmann tensor $\mathcal{T}$ depends on details of the action. See Ref.[15] for the derivation of (26) with the concrete definition of $\mathcal{T}$ and the other details. Once the tensor network representation is obtained, the numerical value of Z is obtained by the Grassmann TRG.

5. Gauge field theory

The tensor network for gauge theory is defined by character expansions (CE). Some models with U(1) and SU(2) have already been studied by the TRG because the CE is easily calculated for these cases. However, for general gauge groups including SU(3), it is not straightforward to calculate the CE. Therefore numerical values of the tensor network cannot be obtained concretely from its formal definition with the CE for general cases. In this section, we review a method of defining a tensor network in two dimensional Yang-Mills theory without the direct use of CE according to Ref.[33]. Hereafter we concentrate on SU(N) gauge group but the method given below can easily be extended to arbitrary compact gauge groups.

The lattice gauge field is given by an SU(N)-valued link field $U_\mu(n)$ which lives on the link $(n, n+\hat{\mu})$. The associated plaquette field is defined as

$$P_{\mu\nu}(n) = U_\mu(n)\, U_\nu(n+\hat{\mu})\, U_\mu^\dagger(n+\hat{\nu})\, U_\nu^\dagger(n), \tag{27}$$

which is covariant under a lattice gauge transformation $U_\mu(n) \to \Lambda(x)U_\mu(n)\Lambda^\dagger(x+\hat{\mu})$. Wilson's plaquette gauge action is then given by

$$S = \frac{\beta}{N}\sum_{n\in\Gamma_2}\sum_{\mu<\nu}\mathrm{Re}\,\mathrm{tr}(1-P_{\mu\nu}(n)). \tag{28}$$

The partition function is

$$Z = \int [dU]\,\mathrm{e}^{-S}, \tag{29}$$

where $[dU] = \prod_{n\in\Gamma_2}\prod_\mu dU_\mu(n)$ with the Haar measure $dU_\mu(n)$.

We now consider the two dimensional case. Then the integrand of (29) is given by the product of $\exp(-\beta/N\,\mathrm{Re}\,\mathrm{tr}(1-P_{12}(n)))$. This factor may be regarded as an infinite dimensional tensor putting on the center of the plaquette:

$$\mathfrak{T}_{u_1u_2u_3u_4} = \exp\left(-\frac{\beta}{N}\mathrm{Re}\,\mathrm{tr}(1-u_1u_2u_3^\dagger u_4^\dagger)\right) \tag{30}$$

where u_i takes any SU(N) value. Thus we find that the partition function is expressed as a tensor network,

$$Z = \mathfrak{T}r\prod_{n\in\Gamma_2}\mathfrak{T}_{g_nh_ng'_nh'_n}. \tag{31}$$

Here g', h' obey the same identification as x', y' of (3) and $\mathfrak{T}r$ denotes the integrations of link fields $g_n \equiv U_1(n)$ and $h_n \equiv U_2(n)$.

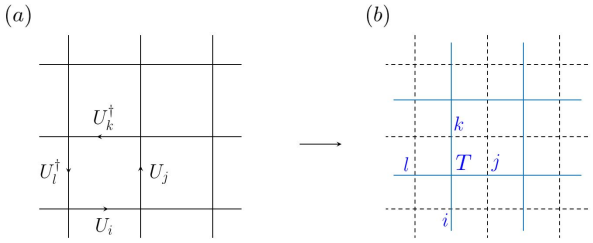

Figure 5: Tensor network representation of 2d Yang-Mills theory.

We now discretize the Haar measure to define a finite dimensional tensor as

$$\int dU\,g(U) \approx \frac{1}{K}\sum_{i=1}^{K} g(U_i), \tag{32}$$

where $\{U_1, U_2, \ldots, U_K\}$ are random $SU(N)$ fields. Instead of (31), using this discretization for all of $dU_\mu(n)$, we have

$$Z \approx \mathrm{Tr}\prod_{n\in\Gamma_2} T_{i_nj_ni'_nj'_n}, \tag{33}$$

where

$$T_{ijkl} = \frac{1}{K^2} e^{-(\beta/N)\,\mathrm{Re\,tr}\,(1-U_i U_j U_k^\dagger U_l^\dagger)} \tag{34}$$

Here Tr denotes the summation over $i_n, j_n = 1, \cdots, K$ for all $n \in \Gamma_2$ under the proper identification of indices. Fig.5 shows the tensor network representation graphically. This representation does not use the CE and the numerical value of (34) is easily obtained. Since the approximated partition function (33) depends on K, we should check the convergence of results with respect to K numerically.

Fig. 6 shows the free energy density $f(\beta) = \log Z/(\beta V)$ and the energy density $e(\beta) = -(1/V)\partial \log Z/\partial\beta$ against K. As can be seen in these figures, as K increases, the numerical results smoothly approach the exact value. We make a χ^2 fit for results at $K = 70, 80, \ldots, 120$ using $g(K) \equiv \mu + \alpha K^{-p}$. Table 1 shows obtained fit results. We find that the extrapolated results to large K are very close to the exact values and our method properly works for SU(3) gauge group.

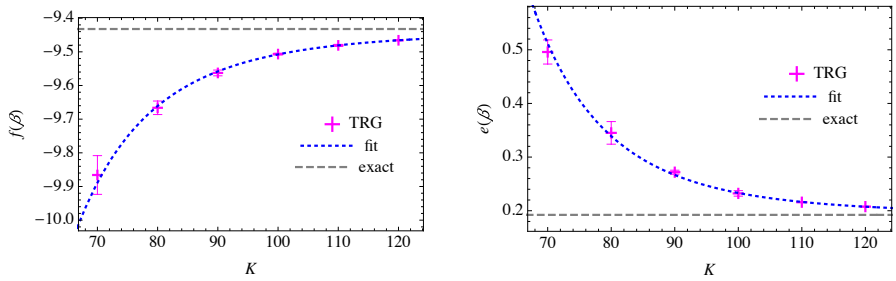

Figure 6: K dependences of $f(\beta)$ (Left) and $e(\beta)$ (Right) with $\beta/V = 0.005$, $V = 64^2$, $D = 90$ for SU(3).

	(exact)	μ	α	p	χ^2/DOF
$f(\beta)$	-9.4323	$-9.4400^{+0.0019}_{-0.0043}$	$-0.3^{+0.2}_{-1.7} \times 10^{10}$	$5.31^{+0.44}_{-0.01}$	0.21
$e(\beta)$	0.1923	$0.1941^{+0.0017}_{-0.0008}$	$2.2^{+5.6}_{-1.6} \times 10^{10}$	$5.88^{+0.29}_{-0.01}$	1.18

Table 1: Results of the χ^2 fit for $SU(3)$.

6. TRG in higher dimensions

Some higher dimensional TRG methods have been proposed so far. The HOTRG[7] is the most famous one which can be applied to any dimension. We firstly review the HOTRG method, after which we will see the triad TRG method[9] in which smaller rank tensors are constituents of a tensor network to reduce the computational cost.

We consider a d-dimensional lattice model with local interactions consisting of bosonic fields since fermions are easily included using the Grassmann tensors. As discussed in the previous sections, we may give a tensor in the form

$$T_{i_1 i_2, \ldots i_{2d}} = \sum_a W^{(1)}_{a i_1} W^{(2)}_{a i_2} \cdots W^{(2d)}_{a i_{2d}}. \tag{35}$$

Here $W^{(m)}_{ai}$ are originated from the hopping terms on $2d$ links. If the theory is invariant under the euclidean group symmetry, the $2d$ hopping terms provide the same W, that is, $W^{(m)} = W$ for $m = 1, 2 \cdots 2d$. Hereafter we focus on the case of $d = 3$. The partition function is then expressed as a tensor network

$$Z = \mathrm{Tr} \prod_{n \in \Gamma_3} T_{x_n y_n z_n x'_n y'_n z'_n}. \tag{36}$$

with the rank-6 tensor (35) for $d = 3$. Here we assume that each tensor index runs from 1 to D.

The renormalization of the HOTRG is carried out for x, y, z directions alternately. It is enough to define the renormalization along z axis. As shown in Fig. 7 (a), we first introduce a rank-10 tensor M as

$$M_{xx'yy'zz'} \equiv \sum_d T_{x_1 y_1 d x'_1 y'_1 z'} T_{x_2 y_2 z x'_1 y'_1 d} \tag{37}$$

where $x = x_1 \otimes x_2$ and $y = y_1 \otimes y_2$ and the same applies to x' and y'. Let us introduce a matrix representation of M as $M'_{x,x'yy'zz'} \equiv M_{xx'yy'zz'}$. Then, we diagonalize a $D^2 \times D^2$ matrix $K_1 \equiv M' M'^{\dagger}$ as

$$K_1 = U \Lambda_1 U^{\dagger} \tag{38}$$

where Λ_1 is a diagonal matrix in which eigenvalues are sorted in the descending order and U is the unitary matrix containing the eigenvectors. Similarly, for the y direction, we have

$$K_2 = V \Lambda_2 V^{\dagger} \tag{39}$$

where $K_2 \equiv M'' M''^{\dagger}$ with a matrix representation as $M''_{y,xx'y'zz'} \equiv M_{xx'yy'zz'}$. U and V can also be obtained from other diagonalizations, and better ones are selected by comparing residuals. See Ref.[7] for the details.

Using two isometries U and V, a renormalized tensor is defined as

$$T'_{xx'yy'zz'} \equiv \sum_{i,j,k,l=1}^{D^2} U^{\dagger}_{xi} V^{\dagger}_{yk} M_{ijklzz'} U_{jx'} V_{ly'}, \tag{40}$$

which is shown in Fig. 7 (b). Here, although x, y, x', y' of T' run from 1 to D^2 originally, we truncate the bond dimension so that all indices runs from 1 to D. Thus Z is again given by the tensor network with the renormalized tensor T'. This completes a renormalization step of the HOTRG.

Repeating the above renormalization for x, y, z axes alternately, we obtain a series of renormalized tensors $T^{(0)} \to T^{(1)} \to T^{(2)} \to \cdots$ starting from the initial tensor $T^{(0)}$. For a periodic lattice of a finite volume $V = 2^{3N} (= 2^N \times 2^N \times 2^N)$ where N is an integer, we finally obtain an approximation of Z as $Z \approx \sum_{x,y,z} T^{(3N)}_{xxyyzz}$. In d dimensions, the HOTRG is formulated in the similar manner. The cost of the HOTRG scales with $O(D^{4d-1})$ which comes from the contractions that make the renormalization tensor.

The reason why the computational cost of the HOTRG is high is that it involves the contraction of two rank $2d$ tensors. If a renormalization group is formulated on a tensor network made only of

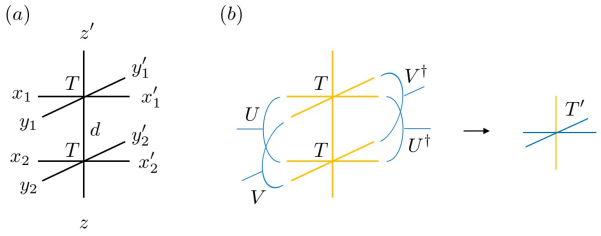

Figure 7: M of the HOTRG (a) and the renormalized tensor (b)

smaller rank tensors, the cost could be naturally reduced. The triad TRG method is created with this kind o idea in the background.

For $d = 3$, without any approximation, the initial tensor (35) can be written in the form

$$T_{ijklmn} = \sum_{a,b,c} A_{ija} B_{akb} C_{blc} D_{cmn}, \tag{41}$$

where

$$A_{ija} = W^{(1)}_{ai} W^{(2)}_{aj}, \tag{42}$$
$$B_{akb} = \delta_{ab} W^{(3)}_{ak}, \tag{43}$$
$$C_{blc} = \delta_{bc} W^{(4)}_{bl}, \tag{44}$$
$$D_{cmn} = W^{(5)}_{cm} W^{(6)}_{cn}. \tag{45}$$

This kind of tensor representation is referred to as a triad representation in this paper. Fig.8 shows this representation.

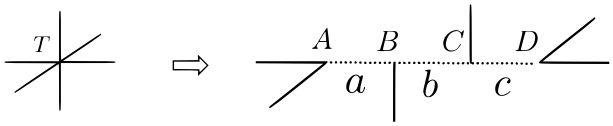

Figure 8: Triad representation (41).

The triad representation is not unique because we have many other decompositions with rank-3 tensors. Of course, there exist mixture representations in which rank-4 and higher rank tensors are used to give the rank $2d$ tensors in d dimensions. Possible representations are shown in Fig.9. The computational cost of the triad TRG is shown to be reduced to $O(D^{d+3})$ in d dimensions with using the randomized singular value decomposition (RSVD). See the appendix A of Ref. [9] for the detail of the RSVD.

In the rest of this section, we explain the triad TRG method for $d = 3$ briefly. Fig.10 shows the evaluation of $K = MM^\dagger$ in the representation. We can evaluate K at a cost of $O(D^6)$. The

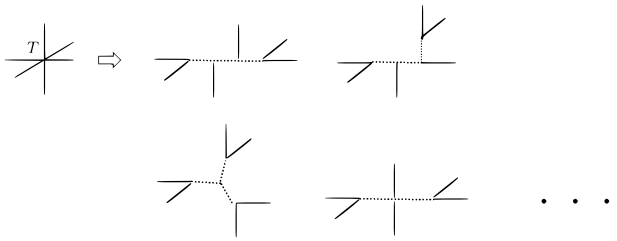

Figure 9: Possible representations of the tensor T.

isometries are obtained at a cost of $O(D^6)$ from the diagonalization of K. These costs are reduced to $O(D^5)$ with the RSVD. The situation does not change for higher dimensions. The cost of making isometries does not depend on the dimensionality and is always $O(D^6)$ ($O(D^5)$ with the RSVD) for any dimension. Once the isometries are obtained, we can create a renormalized triad at a cost of $O(D^6)$ for $d = 3$ with the RSVD. The total cost of the triad TRG becomes $O(D^{d+3})$ in d dimensions. See Ref.[9] for the detail of making the renormalized triads.

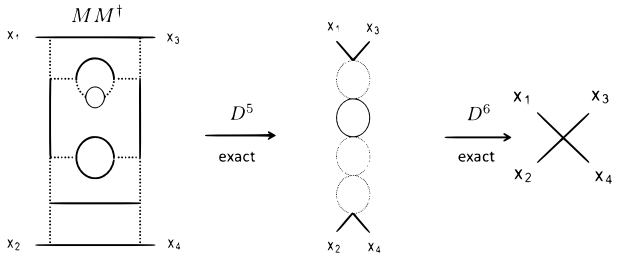

Figure 10: Evaluation of $MM^\dagger$.

The free energy of 3d Ising classical model are obtained by the three TRG methods (HOTRG, ATRG, and the triad TRG) in Ref.[9] The triad TRG method shows a better performance in 3 dimensions.

As shown in Fig11, the error at a fixed computational time depends on a kind of tensor representation. Let N_i be the number of internal indices of a representation such as a, b, c for the representation (41). If N_i is very large, the calculation will be less accurate due to the decomposition corresponding to the internal index, which will increase the error. Conversely, for $N_i \to 0$, the error will increases because the computational cost becomes expensive and we cannot take larger D. Therefore the best one is expected to have intermediate number of internal indices. In the d dimension, identifying the best tensor representation is still an open question.

7. Summary

The TRG method is a very attractive approach as a new calculation method for lattice field theory because it effectively works for theories with the sign problem on extremely large volume

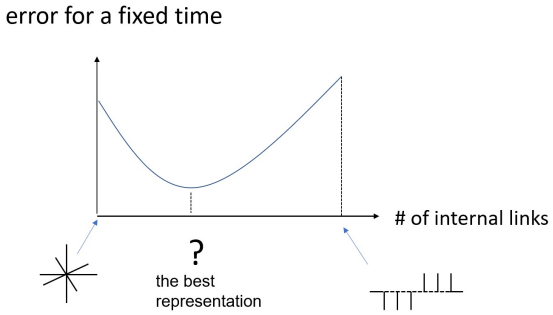

Figure 11: What is the best representation?

lattices. In this paper, I comprehensively reviewed the recent developments in the TRG approach to quantum field theory.

For scalar fields, a finite dimensional tensor is introduced by discretizations of scalar fields. For this, we currently use a one-dimensional quadrature method such as the Gaussian quadrature rule for each measure. In the future, we should develop a discretization method that incorporates the feature of quantum field theory. On the other hand, it is relatively easy to apply the TRG method in a fermion system. The fermionic algorithm of the TRG method is called the Grassmann TRG in which tensor index obeys an anti-commuting rule. The tensor network representation was already obtained for general lattice fermions with a local action.

The tensor network method for gauge theory uses the character expansion. A finite-dimensional tensor has been introduced by truncating the character expansion so far. However, in general gauge groups including SU(3), it remained a difficult issue to numerically calculate the tensor component concretely from the character expansion. Using a new methodology that discretizes the Haar measure with random SU(N) fields, 2d SU(3) Yang-Mills theory was investigated by the TRG. This method may provide hints on the problem to be solved in order to calculate QCD by the TRG method.

Creating a TRG methods in dimensions larger than two is a difficult problem due to the increased computational costs. In fact, the HOTRG method has a calculation cost proportional to $O(D^{4d-1})$. The ATRG method is currently very effective in 4 dimensions. Further improvements are needed to reduce errors. We should look for a renormalization group method that is the best in four dimensions. To do this, the triad TRG method may contain some good ideas.

The most difficult problem that remains would be the development of an effective TRG method in a system with many degrees of freedom, including QCD. Further developments are needed to establish calculation methods in finite density QCD, supersymmetric theory and quantum gravity, and quantum calculation and real-time simulation. The TRG method will greatly develop as a new calculation method for quantum field theory in the next decade.

Acknowledgments

This work was supported by JSPS KAKENHI Grant Numbers JP19K03853, JP21K03537, and JP22H01222. I would like to thank Shinji Takeda, Masafumi Fukuma, Jun Nishimura, Hideaki Oba, Nobuyuki Matsumoto, Hiroto So, and So Matsuura for valuable discussions on tensor networks and related theories. I also would like to thank Noboru Kawamoto for his encouragement.

References

[1] M. Levin and C. P. Nave, *Tensor renormalization group approach to 2D classical lattice models*, *Phys. Rev. Lett.* **99** (2007) 120601, [cond-mat/0611687].

[2] Z. Y. Xie, H. C. Jiang, Q. N. Chen, Z. Y. Weng and T. Xiang, *Second Renormalization of Tensor-Network States*, *Phys. Rev. Lett.* **103** (2009) 160601, [0809.0182].

[3] Y. Nakamura, H. Oba and S. Takeda, *Tensor Renormalization Group Algorithms with a Projective Truncation Method*, *Phys. Rev. B* **99** (2019) 155101, [1809.08030].

[4] D. Kadoh, Y. Kuramashi and R. Ueno, *Irregular parameter dependence of numerical results in tensor renormalization group analysis*, *PTEP* **2019** (2019) 061B01, [1812.10517].

[5] H. Oba, *Cost reduction of the bond-swapping part in an anisotropic tensor renormalization group*, *PTEP* **2020** (2020) 013B02, [1908.07295].

[6] D. Kadoh, H. Oba and S. Takeda, *Triad second renormalization group*, 2107.08769.

[7] Z. Y. Xie, J. Chen, M. P. Qin, J. W. Zhu, L. P. Yang and T. Xiang, *Coarse-graining renormalization by higher-order singular value decomposition*, *Physical Review B* **86** (jul, 2012) .

[8] D. Adachi, T. Okubo and S. Todo, *Anisotropic Tensor Renormalization Group*, *Phys. Rev. B* **102** (2020) 054432, [1906.02007].

[9] D. Kadoh and K. Nakayama, *Renormalization group on a triad network*, 1912.02414.

[10] Z.-C. Gu, F. Verstraete and X.-G. Wen, *Grassmann tensor network states and its renormalization for strongly correlated fermionic and bosonic states*, 1004.2563.

[11] Z.-C. Gu, *Efficient simulation of Grassmann tensor product states*, *Phys. Rev. B* **88** (2013) 115139, [1109.4470].

[12] R. Sakai, S. Takeda and Y. Yoshimura, *Higher order tensor renormalization group for relativistic fermion systems*, *PTEP* **2017** (2017) 063B07, [1705.07764].

[13] Y. Yoshimura, Y. Kuramashi, Y. Nakamura, S. Takeda and R. Sakai, *Calculation of fermionic Green functions with Grassmann higher-order tensor renormalization group*, *Phys. Rev. D* **97** (2018) 054511, [1711.08121].

[14] N. Butt, S. Catterall, Y. Meurice, R. Sakai and J. Unmuth-Yockey, *Tensor network formulation of the massless Schwinger model with staggered fermions*, *Phys. Rev. D* **101** (2020) 094509, [1911.01285].

[15] S. Akiyama and D. Kadoh, *More about the Grassmann tensor renormalization group*, *JHEP* **10** (2021) 188, [2005.07570].

[16] Y. Shimizu, *Tensor renormalization group approach to a lattice boson model*, *Mod. Phys. Lett. A* **27** (2012) 1250035.

[17] Y. Shimizu, *Analysis of the* $(1+1)$*-dimensional lattice* ϕ^4 *model using the tensor renormalization group*, *Chin. J. Phys.* **50** (2012) 749.

[18] D. Kadoh, Y. Kuramashi, Y. Nakamura, R. Sakai, S. Takeda and Y. Yoshimura, *Tensor network analysis of critical coupling in two dimensional* ϕ^4 *theory*, *JHEP* **05** (2019) 184, [1811.12376].

[19] D. Kadoh, Y. Kuramashi, Y. Nakamura, R. Sakai, S. Takeda and Y. Yoshimura, *Investigation of complex* ϕ^4 *theory at finite density in two dimensions using TRG*, *JHEP* **02** (2020) 161, [1912.13092].

[20] M. Campos, G. Sierra and E. Lopez, *Tensor renormalization group in bosonic field theory*, *Phys. Rev. B* **100** (2019) 195106, [1902.02362].

[21] Y. Meurice, *Examples of symmetry-preserving truncations in tensor field theory*, *Phys. Rev. D* **100** (2019) 014506, [1903.01918].

[22] C. Delcamp and A. Tilloy, *Computing the renormalization group flow of two-dimensional* ϕ^4 *theory with tensor networks*, *Phys. Rev. Res.* **2** (2020) 033278, [2003.12993].

[23] Y. Shimizu and Y. Kuramashi, *Grassmann tensor renormalization group approach to one-flavor lattice Schwinger model*, *Phys. Rev. D* **90** (2014) 014508, [1403.0642].

[24] Y. Shimizu and Y. Kuramashi, *Berezinskii-Kosterlitz-Thouless transition in lattice Schwinger model with one flavor of Wilson fermion*, *Phys. Rev. D* **97** (2018) 034502, [1712.07808].

[25] S. Takeda and Y. Yoshimura, *Grassmann tensor renormalization group for the one-flavor lattice Gross–Neveu model with finite chemical potential*, *PTEP* **2015** (2015) 043B01, [1412.7855].

[26] H. Kawauchi and S. Takeda, *Tensor renormalization group analysis of CP(N-1) model*, *Phys. Rev. D* **93** (2016) 114503, [1603.09455].

[27] K. Nakayama, L. Funcke, K. Jansen, Y.-J. Kao and S. Kühn, *Phase structure of the CP(1) model in the presence of a topological* θ*-term*, *Phys. Rev. D* **105** (2022) 054507, [2107.14220].

[28] D. Kadoh, Y. Kuramashi, Y. Nakamura, R. Sakai, S. Takeda and Y. Yoshimura, *Tensor network formulation for two-dimensional lattice $\mathcal{N} = 1$ Wess-Zumino model*, *JHEP* **03** (2018) 141, [1801.04183].

[29] D. Kadoh and K. Nakayama, *Direct computational approach to lattice supersymmetric quantum mechanics*, *Nucl. Phys. B* **932** (2018) 278–297, [1803.07960].

[30] A. Bazavov, S. Catterall, R. G. Jha and J. Unmuth-Yockey, *Tensor renormalization group study of the non-Abelian Higgs model in two dimensions*, *Phys. Rev. D* **99** (2019) 114507, [1901.11443].

[31] Y. Kuramashi and Y. Yoshimura, *Tensor renormalization group study of two-dimensional U(1) lattice gauge theory with a θ term*, *JHEP* **04** (2020) 089, [1911.06480].

[32] M. Asaduzzaman, S. Catterall and J. Unmuth-Yockey, *Tensor network formulation of two dimensional gravity*, *Phys. Rev. D* **102** (2020) 054510, [1905.13061].

[33] M. Fukuma, D. Kadoh and N. Matsumoto, *Tensor network approach to two-dimensional Yang–Mills theories*, *PTEP* **2021** (2021) 123B03, [2107.14149].

[34] M. Hirasawa, A. Matsumoto, J. Nishimura and A. Yosprakob, *Tensor renormalization group and the volume independence in 2D U(N) and SU(N) gauge theories*, *JHEP* **12** (2021) 011, [2110.05800].

[35] L. Hostetler, J. Zhang, R. Sakai, J. Unmuth-Yockey, A. Bazavov and Y. Meurice, *Clock model interpolation and symmetry breaking in O(2) models*, *Phys. Rev. D* **104** (2021) 054505, [2105.10450].

[36] Y. Kuramashi and Y. Yoshimura, *Three-dimensional finite temperature Z_2 gauge theory with tensor network scheme*, *JHEP* **08** (2019) 023, [1808.08025].

[37] J. Bloch, R. G. Jha, R. Lohmayer and M. Meister, *Tensor renormalization group study of the three-dimensional O(2) model*, *Phys. Rev. D* **104** (2021) 094517, [2105.08066].

[38] S. Akiyama, D. Kadoh, Y. Kuramashi, T. Yamashita and Y. Yoshimura, *Tensor renormalization group approach to four-dimensional complex ϕ^4 theory at finite density*, *JHEP* **09** (2020) 177, [2005.04645].

[39] S. Akiyama, Y. Kuramashi and Y. Yoshimura, *Phase transition of four-dimensional lattice $\phi 4$ theory with tensor renormalization group*, *Phys. Rev. D* **104** (2021) 034507, [2101.06953].

[40] S. Akiyama, Y. Kuramashi, T. Yamashita and Y. Yoshimura, *Restoration of chiral symmetry in cold and dense Nambu–Jona-Lasinio model with tensor renormalization group*, *JHEP* **01** (2021) 121, [2009.11583].

[41] S. Akiyama and Y. Kuramashi, *Tensor renormalization group study of (3+1)-dimensional Z_2 gauge-Higgs model at finite density*, 2202.10051.

[42] B. Dittrich, F. C. Eckert and M. Martin-Benito, *Coarse graining methods for spin net and spin foam models*, *New J. Phys.* **14** (2012) 035008, [1109.4927].

[43] B. Dittrich, *From the discrete to the continuous: Towards a cylindrically consistent dynamics*, *New J. Phys.* **14** (2012) 123004, [1205.6127].

[44] B. Dittrich, S. Mizera and S. Steinhaus, *Decorated tensor network renormalization for lattice gauge theories and spin foam models*, *New J. Phys.* **18** (2016) 053009, [1409.2407].

[45] B. Dittrich, E. Schnetter, C. J. Seth and S. Steinhaus, *Coarse graining flow of spin foam intertwiners*, *Phys. Rev. D* **94** (2016) 124050, [1609.02429].

[46] W. J. Cunningham, B. Dittrich and S. Steinhaus, *Tensor Network Renormalization with Fusion Charges—Applications to 3D Lattice Gauge Theory*, *Universe* **6** (2020) 97, [2002.10472].

[47] Y. Meurice, *Accurate exponents from approximate tensor renormalizations*, *Phys. Rev. B* **87** (2013) 064422, [1211.3675].

[48] J. F. Yu, Z. Y. Xie, Y. Meurice, Y. Liu, A. Denbleyker, H. Zou et al., *Tensor Renormalization Group Study of Classical XY Model on the Square Lattice*, *Phys. Rev. E* **89** (2014) 013308, [1309.4963].

[49] Y. Liu, Y. Meurice, M. P. Qin, J. Unmuth-Yockey, T. Xiang, Z. Y. Xie et al., *Exact Blocking Formulas for Spin and Gauge Models*, *Phys. Rev. D* **88** (2013) 056005, [1307.6543].

[50] A. Denbleyker, Y. Liu, Y. Meurice, M. P. Qin, T. Xiang, Z. Y. Xie et al., *Controlling Sign Problems in Spin Models Using Tensor Renormalization*, *Phys. Rev. D* **89** (2014) 016008, [1309.6623].

[51] Y. Meurice, *Discrete aspects of continuous symmetries in the tensorial formulation of Abelian gauge theories*, *Phys. Rev. D* **102** (2020) 014506, [2003.10986].

[52] Y. Meurice, R. Sakai and J. Unmuth-Yockey, *Tensor lattice field theory with applications to the renormalization group and quantum computing*, 2010.06539.

[53] S. Akiyama and Y. Kuramashi, *Tensor renormalization group approach to (1+1)-dimensional Hubbard model*, *Phys. Rev. D* **104** (2021) 014504, [2105.00372].

[54] M. C. Bañuls and K. Cichy, *Review on Novel Methods for Lattice Gauge Theories*, *Rept. Prog. Phys.* **83** (2020) 024401, [1910.00257].

[55] J. I. Cirac and F. Verstraete, *Renormalization and tensor product states in spin chains and lattices*, *J. Phys. A* **42** (2009) 504004, [0910.1130].

[56] Y. Liu, *Renormalization Group and Phase Transitions in Spin, Gauge, and QCD Like Theories*, Ph.D. thesis, Iowa U., 2013. 10.2172/1172585.

[57] R. Orus, *A Practical Introduction to Tensor Networks: Matrix Product States and Projected Entangled Pair States*, *Annals Phys.* **349** (2014) 117–158, [1306.2164].